# Simulations for Maxwell fluid flow past a non-linearly convective heat transfer heated exponentially stretching sheet with nanoparticles and heat sources

# **Dr.JULIE**

Lecturer, Department of Mathematics, Government College for Men, Kurnool, A.P, India

## **ABSTRACT:**

This article addresses steady flow of Maxwell nanofluid induced by an exponentially stretching sheet subject to convective heating. The revised model of passively controlled wall nanoparticle volume fraction is taken into account. Numerical solutions of the arising nonlinear boundary value problem (BVP) are obtained by using MATHEMATICA built-in function bvp4c. Simulations are performed for various values of embedded parameters which include local Deborah number( $\lambda$ ), Prandtl number(Pr), Biot number(Bi),density ratio( $\beta$ ), radiation(Rd),radiation absorption(Q1),Brownian motion parameter(Nb) and thermophoresis parameter(Nt). The results are consistent with the previous studies in some limiting cases. It is found that velocity decreases and temperature increases when the local Deborah number is increased. Moreover the influence of Brownian diffusion on temperature and heat transfer rate is found to be insignificant. Increase in activation energy(E1)/density ratio( $\beta$ )reduces the temperature and actual concentration. Temperature enhances and actual concentration reduces with increase Biot number(Bi).

Key Words: Exponential stretching sheet, Maxwell fluid, Newtonian, cooling, non-lineat convection, thermal radiation, Activation energy, chemical reaction, partial slip

#### 1. INTRODUCTION

Many fluids of industrial importance such as multigrade oils, composite materials, blood, polymers, liquid detergents, fruit juices, printing inks and industrial suspensions exhibit shear-rate dependent viscosity and thus cannot be described by the classical model of Newtonian fluids. In view of flow diversity in nature, various models of non-Newtonian fluids have been proposed by researchers. The upper-convected Maxwell fluid is a class of visco-elastic fluid that can explain characteristics of fluid relaxation time. It excludes complicated effects of shear-dependent viscosity and thus allows one to emphasize the influence of fluid's elasticity on characteristics of its boundary layer. The boundary layer equations governing two-dimensional flow of upper-convected Maxwell fluid were first derived by Harris[1]. Sadeghy et al.[2] discussed flow over a moving flat plate, the so-called Sakiadis flow, considering Maxwell fluid. They derived local similarity solutions by four different approaches and concluded that velocity is a decreasing function of the local Deborah number. Sadeghy et al.[3] also studied stagnation-point flow of upper-convected Maxwell fluid using Chebyshev pseudo-spectral collocation-point method. Kumari and Nath[4] used finite difference method to compute numerical solutions of the boundary value problem arising in mixed convection stagnation-point flow of Maxwell fluid. Hayat et al.[5] obtained homotopy based series solution for stagnation-point flow of Maxwell fluid towards a stretching sheet. After these pioneering works, researchers have widely discussed two-and three-dimensional flows of Maxwell fluids in different geometries (see Aliakbar et al.[6] Raftari and Yildirim[7] Hayat et al.,[8,9], Mukhopadhyay[10], Abel et al.[11], Hayat et al.[12], Shateyi[13] and Mushtaq et al.[14].

The pioneering study of Crane[15] on two-dimensional flow induced by a linearly stretching surface is relevant in diverse industrial processes such as polymer processing,

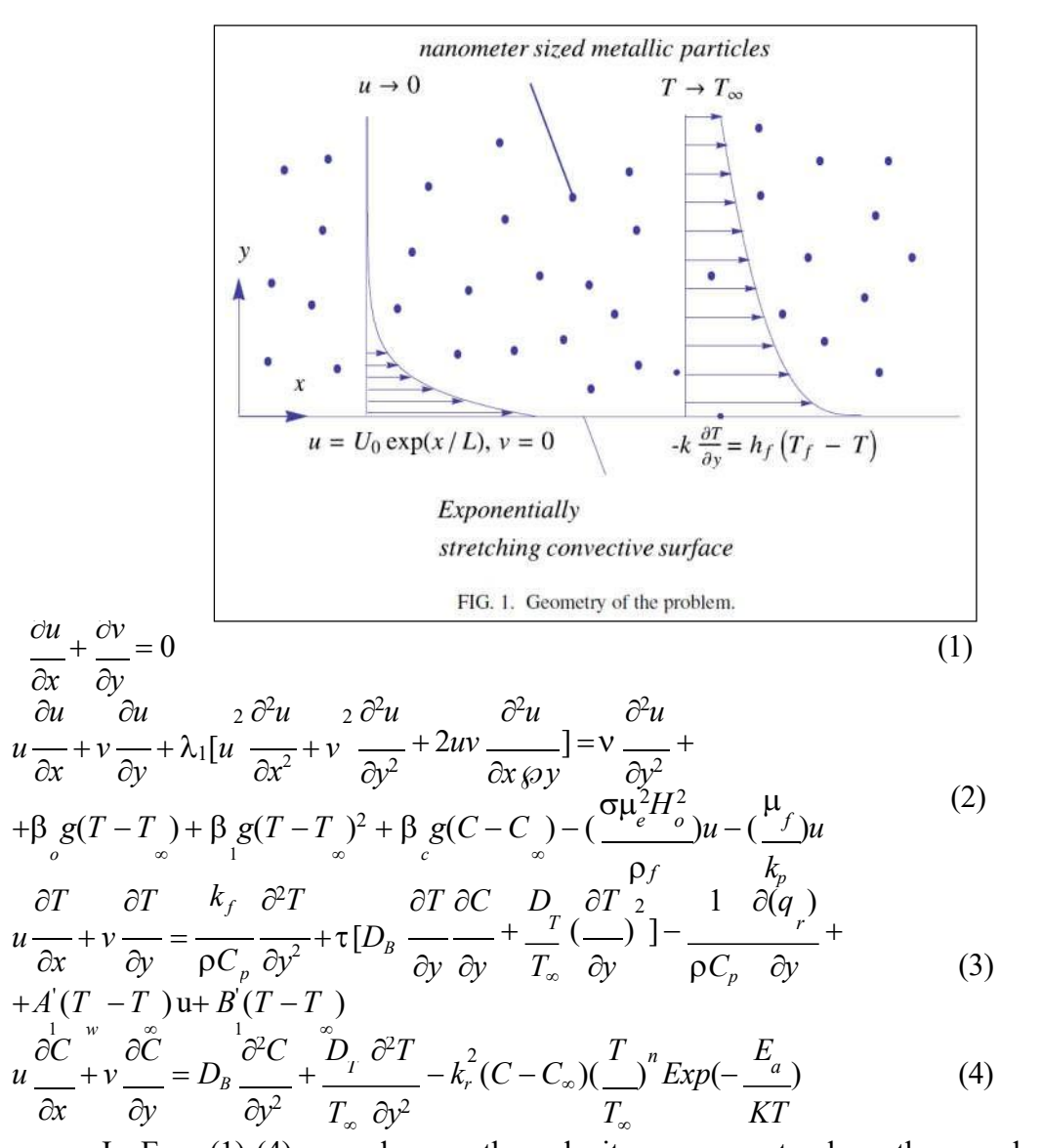
cooling of metallic and rubber sheets, condensation process, crystal growth process etc. In such applications, the velocity of the extruded sheet may not be necessarily linear. Keeping this in view, Magyari and Keller[16] addressed boundary layer flow caused by an exponentially stretching surface. They also examined heat transfer characteristics by considering exponential surface temperature distribution. Elbashbeshy[17] extended this work to a porous stretching sheet. Viscoelastic effects in flow driven by an isothermal exponentially stretching surface were presented by Khan and Sanjayanand.[18] Radiation effects in viscous flow characterized by exponentially stretching surface were analytically investigated by Sajid and Hayat.[19] Recently, flow and heat transfer analyses concerning an exponentially stretching surface have been widely considered by many authors (see Bhattacharyya,[20] Mustafa et al.,[21,22] Liu et al.[23], Abbas et al.[24] Hussain et al.[25].).

Enhanced thermal behavior of nanofluids could provide a basis for innovation in heat transfer intensification, which is of major importance for a number of industrial sectors including transportation, power generation, micro-manufacturing, thermal therapy for cancer treatment, chemical and metallurgical sectors, as well as heating, cooling, ventilation and airconditioning[26].Buongiorno[27]explored that significant improvement in heat transfer processes is the consequence of two main velocity slip effects namely Brownian motion and thermophoretic diffusion of nanoparticles. Kuznetsov and Nield[28] examined heat transfer characteristics in natural convective boundary layer flow of nanofluid past a vertical plate using Buongiorno's model. Nield and Kuznetsov[29] studied the Cheng-Minkowycz problem for natural convective flow past a stationary flat plate immersed in porous medium saturated by nanofluid. The fundamental work on steady boundary layer flow of nanofluid induced by linearly stretching surface was examined by Khan and Pop.[30] They found that thermal boundary layer thickness is an increasing function of both Brownian motion and thermophoresis parameters. Mustafa et al.[31] examined two-dimensional stagnation-point flow towards a stretching sheet, the so called Hiemenz flow, using nanofluid. In another investigation, Mustafa et al.[32] derived both numerical and homotopy solutions for stagnation-point flow of nanofluid caused by exponentially stretching surface. Unsteady flow of nanofluid caused by impulsively stretching plate was addressed by Mustafa et al.[33] Makinde et al[34] explored the problem of Khan and Pop[30] by utilizing convective boundary condition. They observed that intense convective heating at the sheet results in larger temperature and rate of heat transfer from the sheet. During the past few years, flow and heat transfer characteristics in nanofluids have been substantially addressed by researchers (35-46). Recently, Mustafa et al(33a) have studied steady flow of Maxwell nanofluid induced by n exponentially stretching sheet subject to convective heating .The revised model of passively controlled wall nanoparticle volume fraction is considered.

The present study investigates this problem by invoking convective surface boundary condition. Such consideration is important in the sense that base fluids in realistic processes exhibit visco-elastic properties. It has also experimentally proven that de-ionized waternanofluids with poly-ethylene oxide or poly-vinyl-pyrrolidone as a dispersant significantly improved rheological properties in the fluid. Ethylene glycol-Al<sub>2</sub>O<sub>3</sub>, ethylene glycol-CuO and ethylene glycol-ZnO are the examples of visco-elastic nanofluids. Simulations in this study assume that mass flux of nanoparticles at the wall is zero. It is found the self similar solution of the problem is possible only when heat transfer coefficient (associated with the hot fluid below the surface) is proportional to (n-1)/2. The solutions have been computed by using the *MATHEMATICA* built-in routine byp4c and are found in agreement with previous studies in a limiting sense.

#### 2. PROBLEM FORMULATION

Consider steady two-dimensional incompressible flow of Maxwell nanofluid driven by an exponentially stretching sheet aligned with the x- axis as shown in Fig. 1. Let  $U_w(x) =$  $Ue^{x/L}$  be the velocity distribution across the sheet. The temperature at the sheet is controlled by convective process which is characterized by the heat transfer coefficient  $h_f(x)$  and temperature of the hot fluid T<sub>f</sub> below the surface. In accordance with Kuznetsov and Nield [35] we assume zero nanoparticle mass flux at the wall. Let  $T_{\infty}$  be the ambient fluid temperature and  $C_{\infty}$  denotes the nanoparticle volume fraction outside the boundary layer. Using the velocity field V = [u(x, y), v(x, y), 0], the temperature distribution T = T(x, y) and nanoparticle volume fraction distribution C = C(x, y), the boundary layer equations governing the conservations of mass, momentum, energy and nanoparticle mass can be expressed as



In Eqs. (1)-(4), u and v are the velocity components along the x and y directions respectively, v is the kinematic viscosity,  $\lambda_1$  is the relaxation time, T is the fluid temperature, C is the local nanoparticle volume fraction,  $\alpha$  is the thermal diffusivity,  $D_B$  is the Brownian diffusion coefficient,  $D_T$  is the thermophoretic diffusion coefficient and  $\tau = (\rho c)_p/(\rho c)_f$  is the ratio of the effective heat capacity of the nanoparticle material to the effective heat capacity of the fluid.  $\mu$  is the dynamic viscosity, kp is porous permeability coefficient,  $k^2$  is the

(4)

chemical reaction coefficient, K is the Stefan-Boltzmann coefficient, Ea is the activation energy coefficient and qr is the radiative heat flux.

By applying Rosseland approximation (Brewester [7]) the radiative heat flux  $q_r$  is given by

$$q_r = -\left[\frac{4\sigma}{3\beta_R}\right] \frac{1}{\partial y} \left[T'\right] \tag{5}$$

Where  $\sigma^*$  is the Stephan – Boltzmann constant and mean absorption coefficient.

Assuming that the difference in temperature within the flow are such that  $T^{\prime 4}$  can be expressed as a linear combination of the temperature. We expand  $T^{\prime 4}$  in Taylor's series about

Te as follows  $T'^{4} = T^{4} + 4T^{3}(T - T_{0}) + 6T^{2}(T - T_{0}) + \dots$ (6)

Neglecting higher order terms beyond the first degree in  $(T-T_{\infty})$  .we have

$$T^{\prime 4} \cong -3T_0^4 + 4T_0^3 T \tag{7}$$

Differentiating equation (2.6) with respect to y and using (2.8) we get
$$\frac{\partial(q)}{\partial y} = -\frac{16\sigma^* T^3}{3\beta_R} \frac{\partial^2 T}{\partial y^2}$$
(8)

The boundary conditions in the present problem are

$$u = U_{w}(x) = U \exp(x/L) + A' \frac{\partial u}{\partial y}, v = 0,$$

$$-k \int_{f} \frac{\partial T}{\partial y} = h \int_{f} (T_{f} - T), D_{B} \frac{\partial C}{\partial y} + \frac{D_{T}}{T_{\infty}} \frac{\partial T}{\partial y} = 0 \quad at \quad y = 0$$

$$u \to 0, T \to T_{\infty}, C \to C_{\infty} \quad as \quad y \to \infty$$

$$(9)$$

where kf is the thermal conductivity and  $h_f = h \exp(\frac{x}{2I})$  is the heat transfer coefficient.

On using the following similarity variables
$$\eta = (\sqrt{\frac{U}{2\nu L}}) \operatorname{vexp}(\frac{x}{2L}), u = \frac{x}{2L} = -(\sqrt{\frac{v}{2L}}) \operatorname{exp}(\frac{x}{2L}) (f + \eta f'),$$

$$\theta = \frac{T - T_{\infty}}{T_{w} - T_{\infty}}, \phi = \frac{C}{C_{\infty}} \operatorname{exp}(\frac{x}{L}),$$
(10)

Equation(1) is identically satisfied and equations(2-5) reduce to

$$f' - 2(f')^{2} + ff' + \lambda(3fff'' + \frac{\eta}{2}(f')^{2}f' - 0.5f^{2}f' - 2(f')^{3} + \frac{\eta}{2}(f')^{2}f' - \frac{\eta}{2}(f')^{3} + \frac$$

$$+Gr(\theta + \beta\theta^{2} + N\phi) = 0$$

$$(1 + \frac{4Rd}{3})\theta' + \Pr f\theta' + \Pr (Nb\theta'\phi' + Nt\theta'^{2}) + A f' + B\theta = 0$$
(12)

$$\phi' + Scf\phi' + (\frac{Nt}{Nb})\Theta' - \gamma\phi(1 + n\delta\theta)Exp(-\frac{E_1}{1 + \delta\theta}) = 0$$
(13)

$$f(0) = 0, f'(0) = 1 + Af'(0), \theta'(0) = -Bi_1(1 - \theta(0)), Nb\phi'(0) + Nt\theta'(0) = 0,$$
  

$$f'(\infty) \to 0, \theta(\infty) \to 0, \phi(\infty) \to 0$$
where
$$(14)$$

$$Gr = \frac{2\beta_0 L(T_w - T_\infty)}{U^2} \exp(-\frac{2x}{L})$$
 is the Grashof number,  $\lambda = \text{Re}_{x \to 1} \lambda V / 2L^2$  is the local Deborah

number,  $Bi = h/k_f \sqrt{2vL/U}$  is the Biot number,  $Nb = \frac{\tau D_B C_\infty}{V}$  is the Brownian motion

parameter,  $Nt = \frac{\tau D_T (T_f - T_{\infty})}{T_{\infty} V}$  is the thermophoresis parameter,

$$\beta = \frac{\beta_1(T_w - T_\infty)}{\beta_o}, non-linear density \ ratio \ , \ N_r = \frac{\beta_c(C_w - C_\infty)}{\beta_o(T_w - T_\infty)}, buoyancy \ ratio \ ,$$

$$A = \frac{UA'Exp(\frac{x}{L})}{2vL}$$
 is the slip parameter,  $Pr = \frac{\mu C_p}{k_f}$  is the Prandtl number,  $Sc = \frac{v}{D_B}$  is the Schmidt number.

Schmidt number,  $A_{11} = 2A'L$ , is the space dependent heat source parameter,

$$B_{11} = \frac{2LB'}{U} \exp(-\frac{x}{L})$$
 is the heat generating source parameter,  $Rd = \frac{4\sigma \cdot T^3}{k_f \beta_R}$  is the radiation

parameter,  $\gamma = \frac{k_r^2}{v}$  is the chemical reaction parameter,  $\theta_w = \frac{T_w}{T}$ ,  $\delta = \theta_w - 1$  is the

temperature difference parameter,  $E_1 = \frac{E_a}{KT}$  is the activation energy parameter,

Physical quantity of interest in this study is the local

Nusselt number Nux defined as

$$Nux = \frac{xq_w}{k_f(T_f - T_\infty)} \qquad q_w = -k_f \left(\frac{\partial T}{\partial y}\right)_{y=0}$$

where  $\text{Re}_{x} = 2Ue^{(x/L)}L/v$  is the local Reynolds number. It should be noted that reduced Sherwood number which is the dimensionless mass flux is identically zero.

## 3. NUMERICAL RESULTS AND DISCUSSION

Numerical solutions of the boundary value problems given in Eqs. (7)-(10) have been obtained by using the MATLAB built in function byp4c. First of all we compare our results of  $\theta'(0)$  with those of Magyari and Keller[16] and Abbas et al.[24] in limiting cases. The solutions are found in excellent agreement as can be seen from Table I. This gives us confidence that our results are accurate and more general than previously reported studies. In Table II, we provide a sample of our results for reduced Nusselt number  $-\theta'(0)$  corresponding to different values of  $\gamma$  and  $\lambda$  with other parameters fixed. We found that stronger convective heating results in larger magnitude of reduced Nusselt number. However magnitude of reduced Nusselt number is a decreasing function of local Deborah number  $\lambda$ .

TABLE I. Comparison of values for  $\theta'(0)$  with Magyari and Keller  $^{16}$  and Abbas et al.  $^{24}$  in the case of regular fluid.

	$\lambda = 0$	$\lambda = 0.5$		
Pr	Magyari and Keller <sup>16</sup>	Present	Abbas et al. <sup>24</sup>	Present
0.5	-0.330493	-0.330493	-0.175942	-0.301698
1	- 0.549643	- 0.549642	- 0.512337	- 0.512078
3	-1.122188	-1.122077	-1.074513	-1.074501
5	- 1.521243	- 1.521222	- 1.470621	- 1.47060
8	-1.991847	-1.991805	-1.939103	-1.93907
10	- 2.257429	- 2.257381	- 2.203874	- 2.20383

TABLE II. Values of reduced Nusselt number  $-\theta'(0)$  for different values of  $\gamma$  and  $\lambda$  when Pr = 10, Sc = 20 and Nt = Nb = 0.5

$\lambda \setminus \gamma$	0.1	0.5	1	2	5	10
0	0.095615282	0.39606233	0.62184538	0.8081829	0.91441581	0.94117195
0.5	0.095506377	0.39336962	0.61264612	0.78743758	0.88368911	0.90767901
1	0.095412876	0.39105294	0.60480027	0.7702038	0.85877696	0.88069131
1.5	0.095329259	0.3889778	0.59783014	0.75523798	0.83757471	0.85783446

In this analysis we made an attempt to explore the combined influence of activation energy, convectively heated flow of a Maxwell fluid past stretching sheet in the presence of heat sources. The non-linear coupled equations have been solved by using Runge-Kutta fourth order along with Shooting technique. The effect of different governing parameters, viz., Grashof number(G), Magnetic parameter(M), heat source parameters(A1,B1), buoyancy ratio(Nr), Brownian motion parameter(Nb), thermophoresis parameter(Nt), activation energy (E1), temperature difference parameter( $\delta$ ), chemical reaction parameter( $\gamma$ ), radiation parameter(Rd), Convective heat transfer parameter(Bi), non-linear density ratio( $\beta$ ), Schmidt number(Sc), Deborah number( $\lambda$ ) and Prandtl number(Pr). The results have been compared with Mustafa et al(36) with Gr=0,Nr=0,A1=B1=0,O1=0,E1=0, $\delta$ =0, $\gamma$ =0.

Figs.2a-2c depict the variation of axial velocity(f'), temperature ( $\theta$ ) and concentration( $\phi$ ) with Grashof number(Gr) and magnetic parameter(M). From the profiles we find that the velocity enhances and temperature reduces with increase in G. The concentration is negative for all variations. We follow the convention that the non-dimensional concentration is positive/negative according as the actual concentration (C) is greater/lesser than the ambient concentration ( $C_{\infty}$ ). Increase in Gr enhances the actual concentration in the flow region. With respect to magnetic parameter (M) we notice a depreciation in the velocity, actual concentration and upsurge in the temperature with rising values of M(figs.2a-2c).

Figs.3a-3c represent  $f',\theta,\phi$  with buoyancy ratio(Nr) and slip parameter(A). When the molecular buoyancy force dominates over the thermal buoyancy force the velocity, actual concentration enhance, temperature diminishes when the buoyancy forces are in the same direction. An increase in slip parameter (A) leads to a decay in f', actual concentration and enhancement in temperature in the boundary layer flow.

Figs.4a-4c&5a-5c exhibit the variation of  $f',\theta,\phi$  with space/temperature dependent heat source parameters(A1,B1). For larger values of space/temperature dependent heat source (A1>0,B1>0) larger the velocity, temperature and smaller the actual concentration, while an opposite nature is observed in  $f',\theta,\phi$  with space dependent heat sink/heat absorbing source.

Figs.6a-6c demonstrate the variation of  $f',\theta,\phi$  with radiation parameter(Rd) and radiation absorption parameter(Q1). From the profiles we find that the velocity, temperature decay ,actual concentration grows with higher thermal radiation. Increase in radiation absorption (Q1) leads to a rise in velocity, temperature and decay in actual concentration in the flow region.

Figs.7a-7c represent  $f',\theta,\varphi$  with Schmidt number(Sc) and Deborah number( $\lambda$ ). Deborah number is a dimensionless variable that deals with the relaxation time i.e., time taken by the fluid to obtain equilibrium in response to the applied stress. Fluids with small Dedorah displays liquids-like behaviour whereas larger Deborah number corresponds to solid-like substances. An increase in  $\lambda$  corresponds to an increase in fluid viscosity which enhances resistance to flow and hence velocity decrease Further ,with an increase in  $\lambda$ , the profiles approach zero at smaller distances from the surface indicating a reduction in the thickness of the momentum boundary layer. An increase in Deborah number ( $\lambda$ ) decays actual concentration and upsurges the temperature in the flow region. Thus increase in  $\lambda$  leads to growth in thermal boundary layer thickness. With respect to Schmidt number (Sc) we find that lesser the molecular diffusivity smaller the velocity, temperature and larger the actual concentration in the flow region.

An increase in chemical reaction parameter( $\gamma$ ) augments the velocity, temperature and shrinks the actual concentration in the degenerating chemical reaction case while in generating chemical reaction case, velocity, actual concentration enhance, temperature diminishes in the flow region (figs.8a-8c).

The effect of Brownian motion and thermophoresis (Nb, Nt) on flow variables can be seen from figs.9a-9c. Higher the Brownian motion(Nb) smaller the velocity, temperature and larger the actual concentration while a reversed effect is noticed with thermophoresis (Nt).

An increase in activation energy parameter(E1)diminishes the velocity, temperature and enhances the actual concentration .We notice a reversed effect in  $f',\theta,\phi$  with rising values of temperature difference ratio( $\delta$ )(figs.10-10c).

Figs.11a-11c exhibit variation of  $f',\theta,\phi$  with Biot number(Bi) and non-linear density ratio( $\beta$ ). Higher the Biot number(Bi) /larger the velocity, temperature and smaller the actual temperature in the flow region. Increase in non-linear density ratio( $\beta$ ) larger the velocity, actual concentration ,smaller the temperature in the flow region. This indicates that increase in Biot number results in growth of thermal boundary layer thickness.

Figs,12a-12c represent  $f',\theta,\phi$  with Prandtl number(Pr) and index number(n). From the profiles we find that lesser the thermal diffusivity larger the velocity, temperature and smaller the actual concentration in the flow region. Increase in index parameter(n) leads to a depreciation in velocity, actual concentration and growth in temperature in the flow region.

The skin friction, rate of heat and mass transfer on the wall  $\eta$ =0 are exhibited in table.2 for different variations of G,M,Nr,A,Nb,Nt,Rd,A1,B1, $\gamma$ , $\lambda$ ,E1, $\delta$ ,Sc,Q1,Bi,n, $\beta$  and Pr. From the tabular values ,we find that increase in G,Nr grow rate of heat and mass transfer, reduces skin friction on the wall. Skin friction increases, Nu and Sh reduce with rising values of M and  $\lambda$ . Higher Brownian motion leads to increase in skin friction, Nu and reduction in Sh while an increase in thermophoresis (Nt) results in enhancement in skin friction, Sh and depreciation in Nu. Skin friction, Nu and Sh decay with higher values of A, n, space dependent heat source(A1>0) and  $\gamma$ . Higher the radiation(Rd) / activation energy(E1)/ radiation absorption(Q1)/ Schmidt number(Sc)/heat absorbing source(B1<0) grows skin friction, Nu and Sh on  $\eta$ =0.Increase in space dependent heat source(A1<0)/generating heat source (B1>0) decays skin friction, upsurges Nu and Sh. For higher values of Biot

number(Bi) and non-linear density  $ratio(\beta)$ ,we notice a reduction in skin friction, growth in Nu and Sh on the wall  $\eta=0$ .

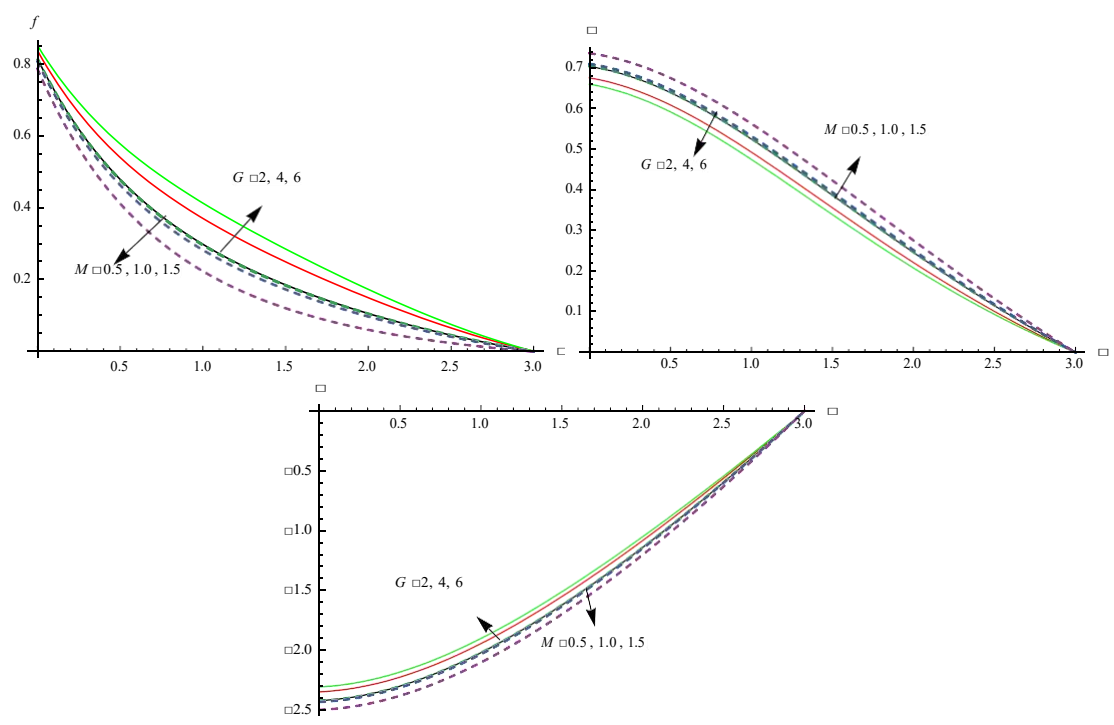


Fig.2 Variation of [a] Velocity(f'),[b]Temperature( $\theta$ ), [c] Concentration(C) with G & M Nr=.2,A=0.2,A11=0.2,B11=0.2,Rd=Q1=0.5,Sc=0.24, $\lambda$ =0.1, $\gamma$ =0.5, Nb=Nt=0.2,E1=0.1, $\delta$ =0.2,Bi=0.1, $\beta$ =0.2,n=0.2,Pr=0.71

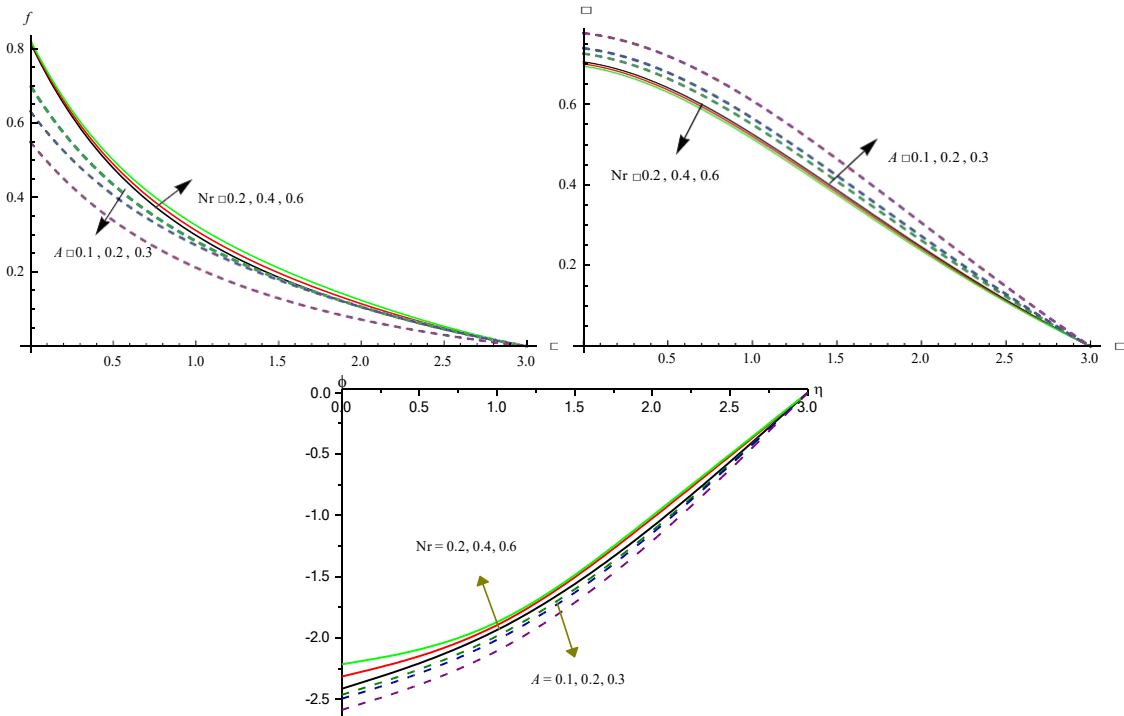


Fig.3 Variation of [a] Velocity(f'),[b]Temperature( $\theta$ ), [c] Concentration(C) with Nr,A G=2,M=0.2,A11=0.2,B11=0.2,Rd=Q1=0.5,Sc=0.24, $\lambda$ =0.1, $\gamma$ =0.5, Nb=Nt=0.2,E1=0.1, $\delta$ =0.2,Bi=0.1, $\beta$ =0.2,n=0.2,Pr=0.71

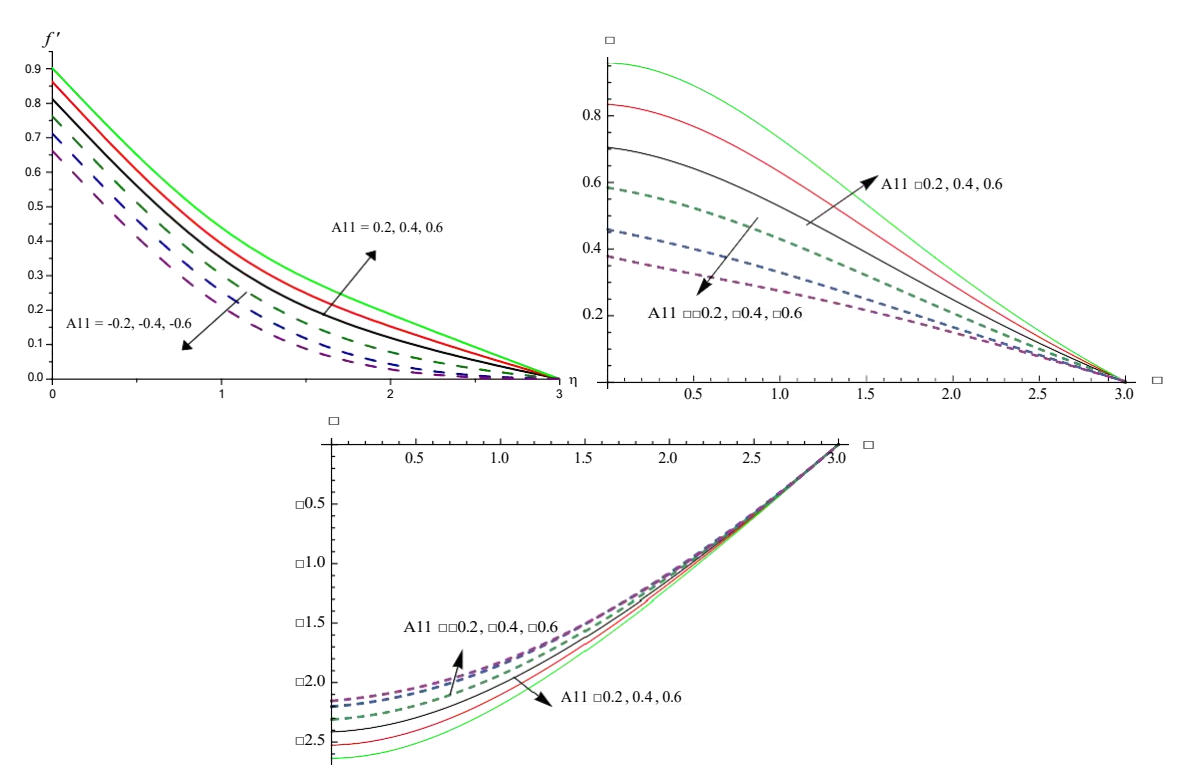


Fig.4 Variation of [a] Velocity(f'),[b]Temperature( $\theta$ ), [c] Concentration(C) with A11 G=2,M=0.2;Nr=.2,A=0.2,B11=0.2,Rd=Q1=0.5,Sc=0.24, $\lambda$ =0.1, $\gamma$ =0.5,Nb=Nt=0.2,E1=0.1, $\delta$ =0 .2,Bi=0.1, $\beta$ =0.2,n=0.2,Pr=0.71

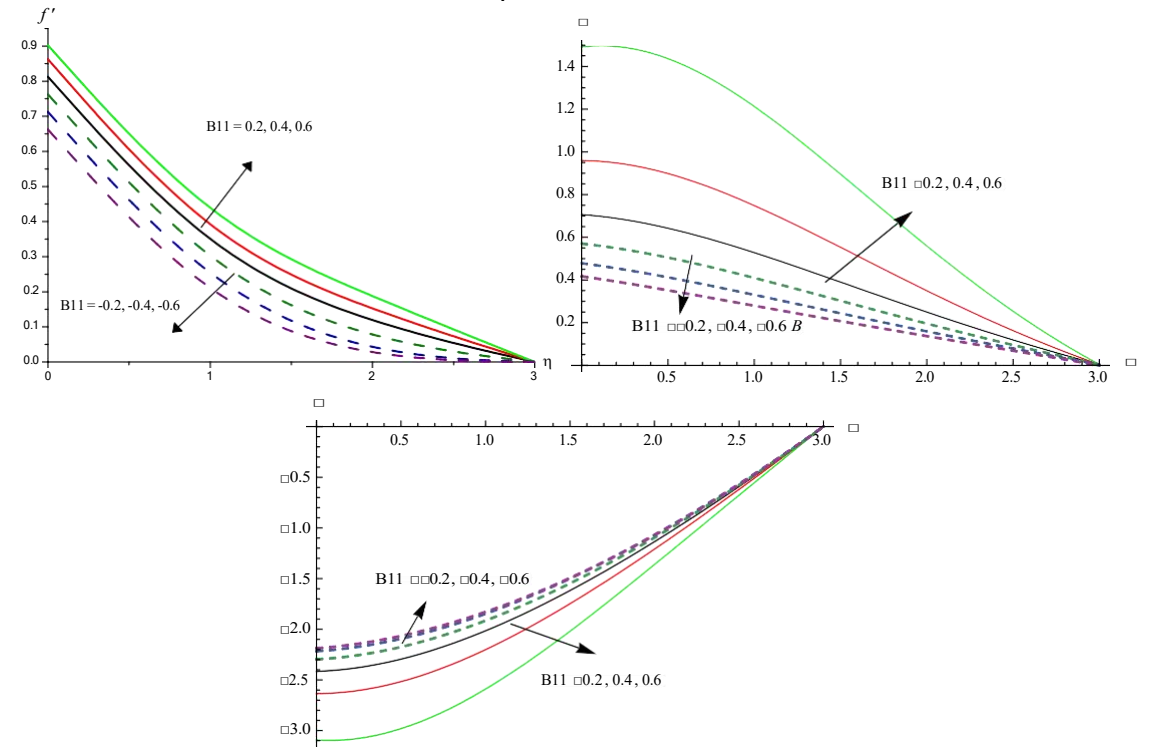


Fig.5 Variation of [a] Velocity(f'),[b]Temperature( $\theta$ ), [c] Concentration(C) with B11 G=2,M=0.2;Nr=.2,A=0.2,A11=0.2,Rd=Q1=0.5,Sc=0.24, $\lambda$ =0.1, $\gamma$ =0.5,Nb=Nt=0.2,E1=0.1, $\delta$ =0 .2,Bi=0.1, $\beta$ =0.2,n=0.2,Pr=0.71

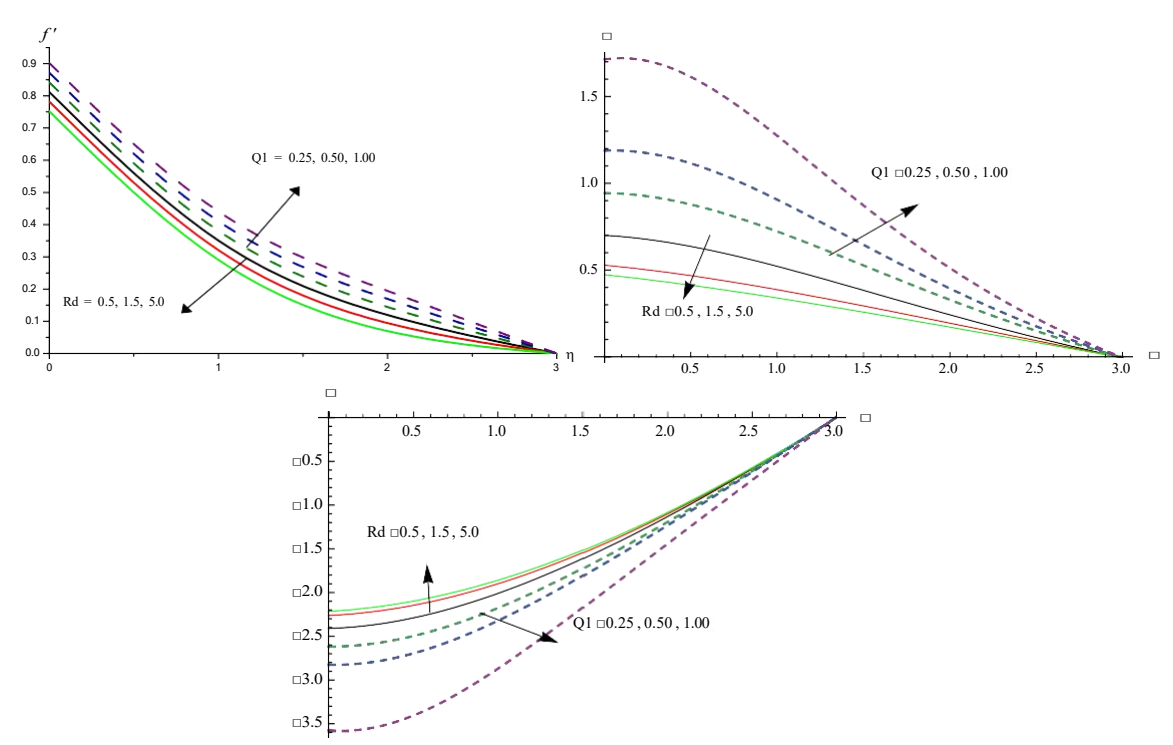


Fig.6 Variation of [a] Velocity(f'),[b]Temperature( $\theta$ ), [c] Concentration(C) with Rd,Q1 G=2,M=0.2,Nr=.2,A=0.2,A11=0.2,B11=0.2,Sc=0.24, $\lambda$ =0.1, $\gamma$ =0.5, Nb=Nt=0.2,E1=0.1, $\delta$ =0.2,Bi=0.1, $\beta$ =0.2,n=0.2,Pr=0.71

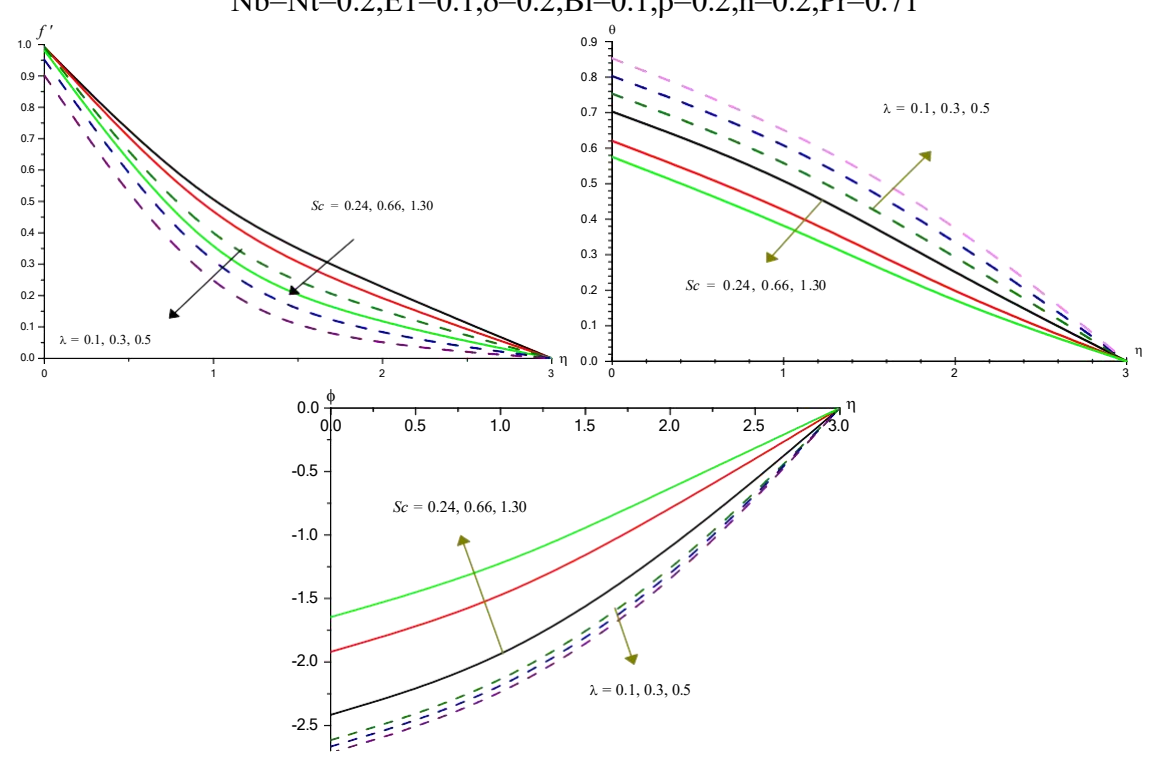


Fig.7 Variation of [a] Velocity(f'),[b]Temperature( $\theta$ ), [c] Concentration(C) with Sc, $\lambda$  G=2,M=0.2,Nr=.2,A=0.2,A11=0.2,B11=0.2,Rd=Q1=0.5, $\gamma$ =0.5, Nb=Nt=0.2,E1=0.1, $\delta$ =0.2,Bi=0.1, $\beta$ =0.2,n=0.2,Pr=0.71

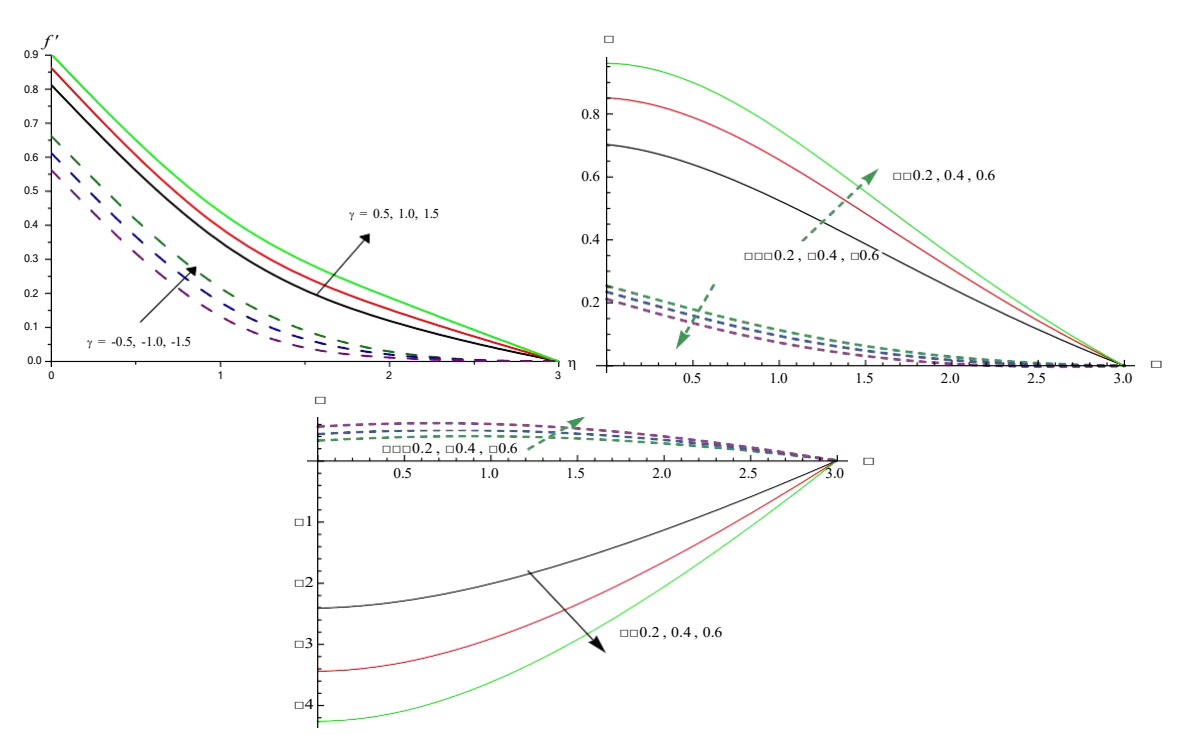


Fig.8 Variation of [a] Velocity(f'),[b]Temperature(θ), [c] Concentration(C) with γ G=2,M=0.2,Nr=.2,A=0.2,A11=0.2,B11=0.2,Rd=Q1=0.5,Sc=0.24,  $\lambda$ =0.1,Nb=Nt=0.2,E1=0.1, $\delta$ =0.2,Bi=0.1, $\beta$ =0.2,n=0.2,Pr=0.71

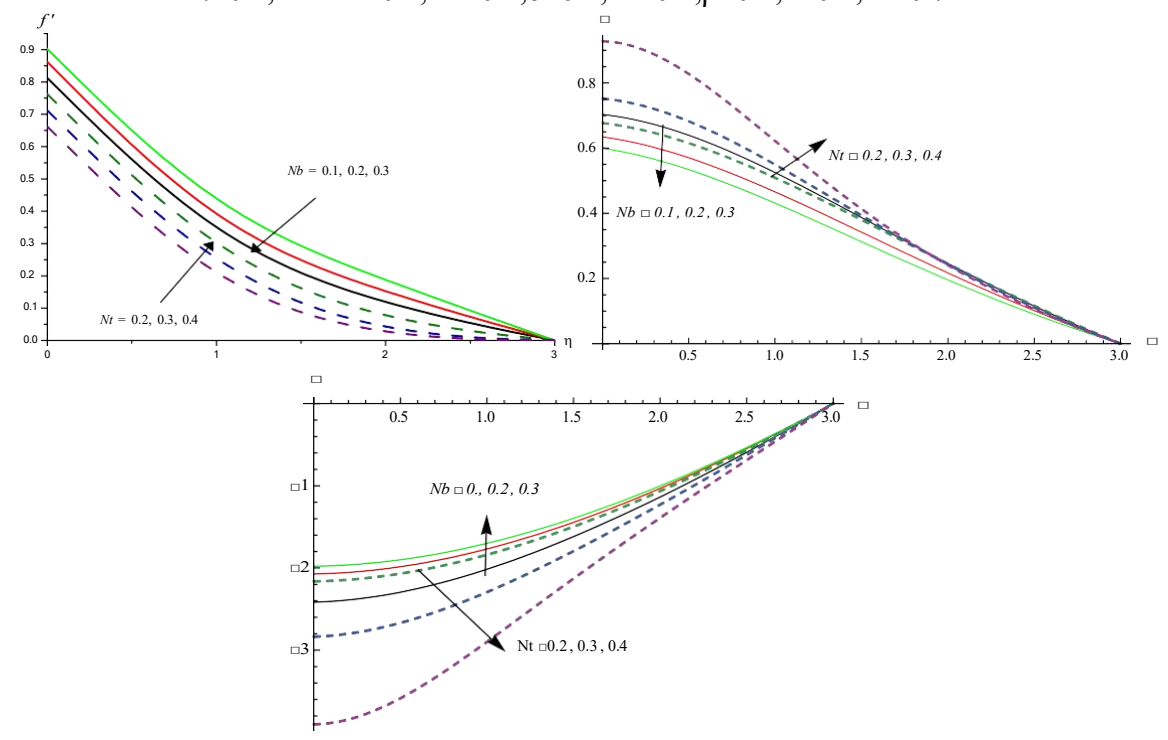


Fig.9 Variation of [a] Velocity(f'),[b]Temperature(θ), [c] Concentration(C) with Nb,Nt G=2,M=0.2,Nr=.2,A=0.2,A11=0.2,B11=0.2,Rd=Q1=0.5,Sc=0.24,  $\lambda$ =0.1, $\gamma$ =0.5,E1=0.1, $\delta$ =0.2,Bi=0.1, $\beta$ =0.2,n=0.2,Pr=0.71

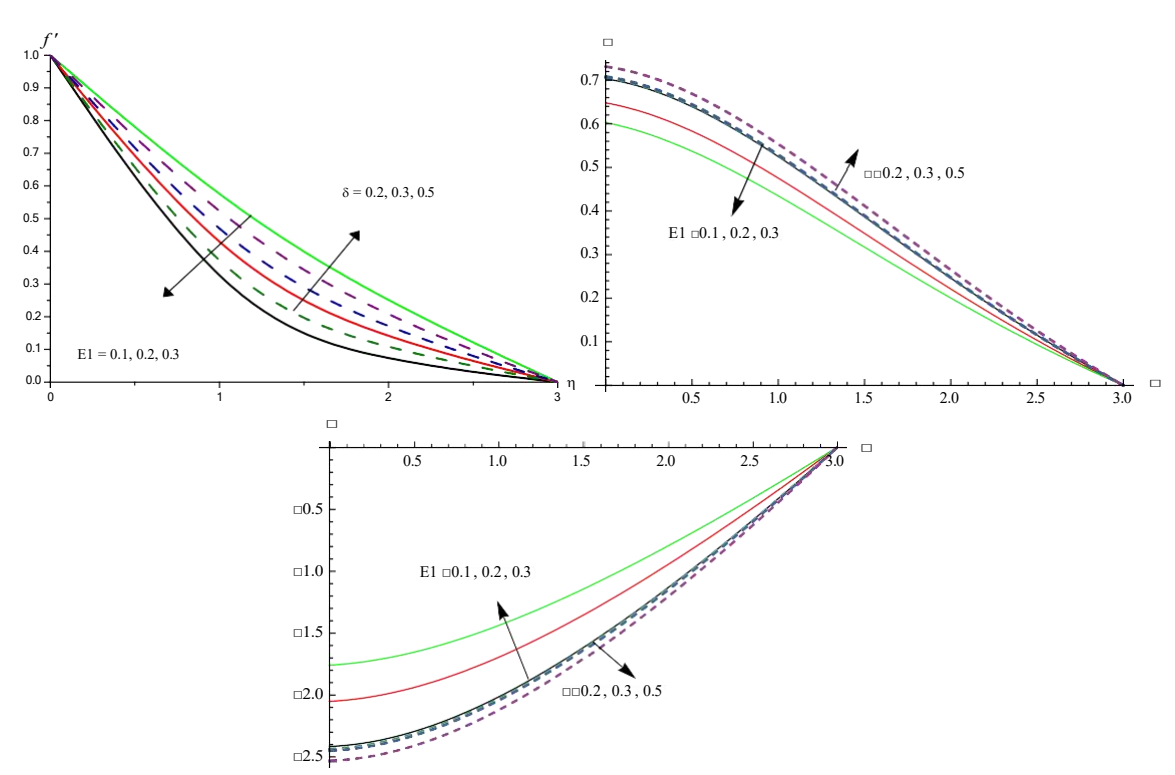


Fig.10 Variation of [a] Velocity(f'),[b]Temperature(θ), [c] Concentration(C) with E1,δ G=2,M=0.2,Nr=.2,A=0.2,A11=0.2,B11=0.2,Rd=Q1=0.5,Sc=0.24,  $\lambda$ =0.1, $\gamma$ =0.5,Nb=Nt=0.2,Bi=0.1, $\beta$ =0.2,n=0.2,Pr=0.71

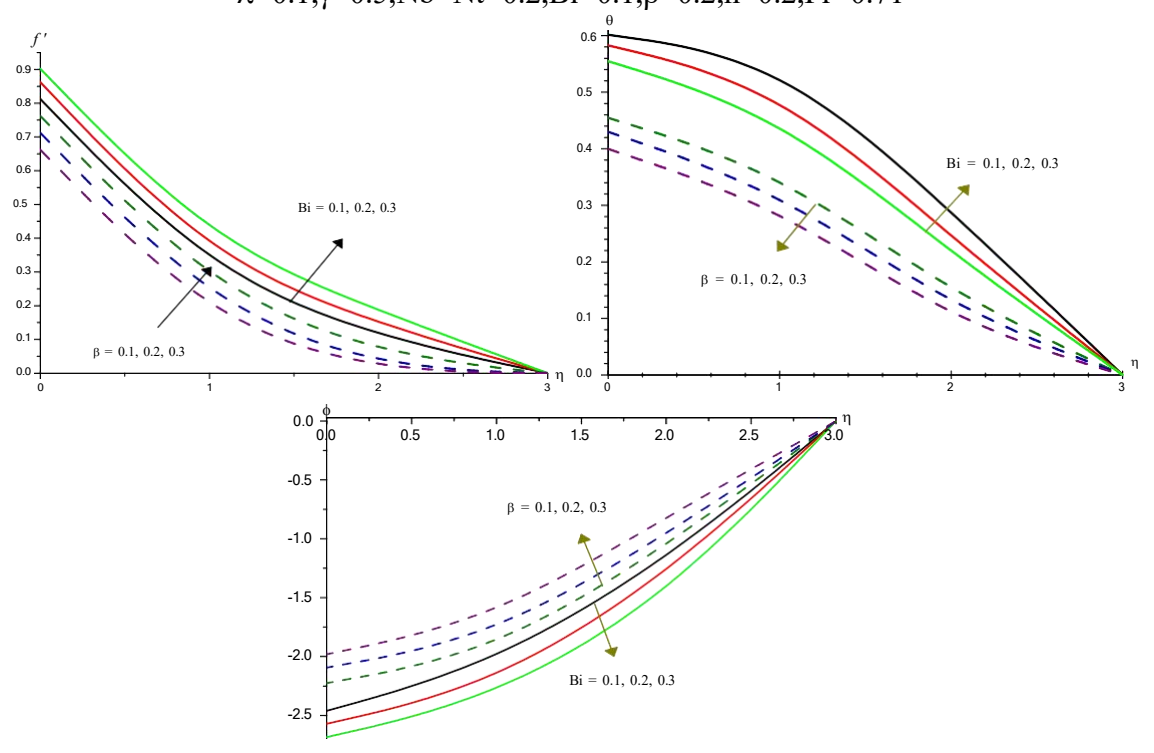


Fig.11 Variation of [a] Velocity(f'),[b]Temperature(θ), [c] Concentration(C) with Bi,β G=2,M=0.2,Nr=.2,A=0.2,A11=0.2,B11=0.2,Rd=Q1=0.5,Sc=0.24,  $\lambda$ =0.1, $\gamma$ =0.5,Nb=Nt=0.2,E1=0.1, $\delta$ =0.2, n=0.2,Pr=0.71

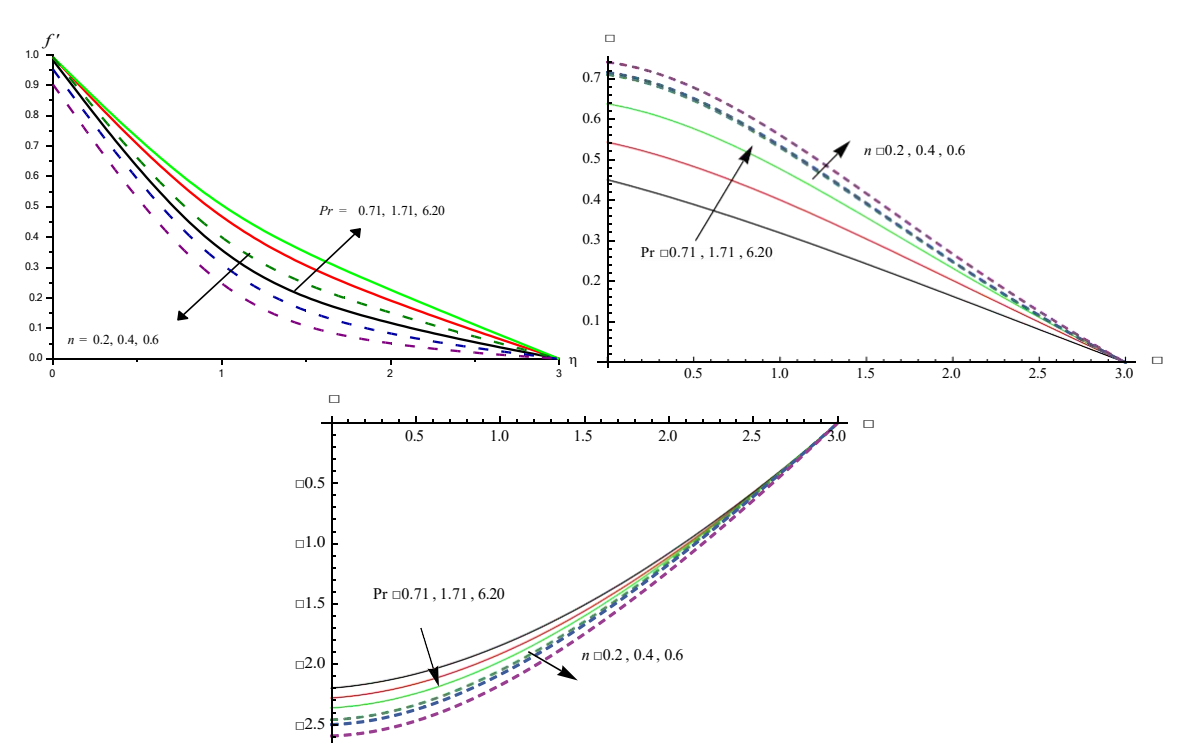


Fig.12 Variation of [a] Velocity(f'),[b]Temperature( $\theta$ ), [c] Concentration(C) with n, Pr G=2,M=0.2,Nr=.2,A=0.2,A11=0.2,B11=0.2,Rd=Q1=0.5,Sc=0.24,  $\lambda$ =0.1, $\gamma$ =0.5,Nb=Nt=0.2,E1=0.1, $\delta$ =0.2,Bi=0.1, $\beta$ =0.2

Para	meter	Cf(0)	Nu(0)	Sh(0)	Parai	neter	Cf(0)	Nu(0)	Sh(0)
G	2	-0.937896	0.0593822	-0.0593822	Nb	0.1	-0.937896	0.0593822	-0.0593822
	4	-0.824976	0.0649549	-0.0649549		0.2	-0.94514	0.0731304	-0.034824
	6	-0.752386	0.0680436	-0.0680436		0.3	-0.948132	0.0800858	-0.0258341
M	0.5	-0.941964	0.0592155	-0.0592155	Nt	0.2	-0.941647	0.0646435	-0.0387861
	1	-0.970011	0.0580651	-0.0580651		0.3	-0.961738	0.0496459	-0.0794335
	1.5	-1.07057	0.0528414	-0.0528414		0.4	-1.00094	0.0144722	-0.0976277
Nr	0.2	-0.937896	0.0593822	-0.0593822	A11	0.2	-0.937896	0.0593822	-0.0594822
	0.4	-0.919132	0.0604163	-0.0604163		0.4	-0.930109	0.0335919	-0.0336919
	0.6	-0.898778	0.0615043	-0.0615043		0.6	-0.928448	0.00865151	-0.00875151
Α	0.1	-0.719282	0.0552998	-0.0552998		-0.2	-0.945115	0.0835804	-0.0835954
	0.2	-0.597521	0.0526372	-0.0526372		-0.4	-0.952495	0.108615	-0.108915
	0.4	-0.551754	0.0451989	-0.045989		-0.6	-1.0087	0.124623	-0.124723
Rd	0.5	-0.937896	0.0593822	-0.0593822	B11	0.2	-0.937896	0.0593822	-0.0594822
	1.5	-0.947901	0.0937474	-0.0937474		0.4	-0.921823	0.0880755	-0.0882755
	5	-0.951287	0.104664	-0.104664		0.6	-0.893783	-0.0975019	0.0975419
Q1	0.5	-0.922934	0.0109056	-0.0109056		-0.2	-0.946395	0.0866174	-0.0866474
_	1	-0.938407	-0.0378618	0.0378618		-0.4	-0.952058	0.1055678	-0.105789
	1.5	-0.953538	-0.142775	0.142775		-0.6	-1.00773	0.116578	-0.116578
E1	0.1	-0.937896	0.0593822	-0.0593822	γ	0.5	-0.937896	0.0593822	-0.0593822
	0.2	-0.945232	0.0703955	-0.0703955		1	-0.917846	0.0298163	-0.0298163
	0.3	-0.951183	0.0794116	-0.0794116		1.5	-0.90253	0.00780788	-0.00780788
δ	0.2	-0.937496	0.0587745	-0.0587745		-0.5	-0.995703	0.149183	-0.149183
	0.3	-0.938172	0.0582834	-0.0582834		-1	-0.998119	0.153075	-0.153075
	0.4	-0.99487	0.0537583	-0.0537583		-1.5	-1.084763	0.157647	-0.157649
Sc	0.2	-0.937896	0.0593822	-0.0593822	β	0.1	-0.935952	0.0594664	-0.0594664
	0.7	-0.949296	0.0759043	-0.0759043		0.2	-0.934191	0.0595424	-0.0595424
	1.3	-0.955455	0.0849232	-0.0849232		0.3	-0.930322	0.0597088	-0.0597088
λ	0.2	-0.951287	0.0589767	-0.0589767	n	0.2	-0.93711	0.0581871	-0.0581871
	0.4	-0.965894	0.0585363	-0.0585363		0.4	-0.936352	0.0570347	-0.0570347
	0.6	-1.02952	0.0549465	-0.0549465		0.6	-0.995124	0.0520814	-0.0520814
Bi	0.2	-0.937896	0.0593822	-0.0593822	Pr	0.7	-0.952955	0.109952	-0.109952
	0.4	-0.934633	0.0950902	-0.0950902		1.7	-0.947203	0.0914622	-0.0914622
	0.6	-0.932766	0.115467	-0.115467		6.2	-0.941589	0.0725508	-0.0725508

#### 4. CONCLUSIONS

We investigated steady convective heat transfer boundary layer flow of Maxwell fluid past an exponentially stretching sheet with nanoparticles. Activation energy, radiation, heat sources, Brownian motion and thermophoresis effects were considered. Further the revised model of passively controlled wall nanoparticle volume fraction was adopted. Numerical solutions were obtained and these were found in agreement with the existing studies. Following are key points of this work.

- 1. Increase in Grahof number enhances the velocity, actual concentration and reduces the temperature .The rate of heat and mss transfer experience growth with increase in G. Higher the Lorentz force smaller the velocity, actual concentration and larger temperature .Skin friction enhances Nu and Sh reduce with M on the wall.
- 2. Higher the thermal radiation (Rd) smaller velocity, temperature and larger actual concentration. Increase in slip parameter(A)enhances the temperature and reduces the velocity, actual concentration. Nu and Sh grow with Rd and decay with increasing values of A. The velocity, actual concentration enhance, temperature reduces with buoyancy ratio(Nr). Skin friction reduces, Nu and Sh grow with Nr on  $\eta$ =0. The non-linearity in density ratio( $\beta$ ) upsurges the temperature and the rate of heat transfer.
- 3. Hgher the activation energy(E1) smaller the velocity, temperature and larger the actual concentration. Skin friction, Nu and Sh grow with E1 on the wall. Temperature difference parameter (δ) exhibits an opposite effect on flow variables (Nu,Sh)
- 4. Hydrodynamic boundary layer becomes thinner and thermal boundary layer becomes thicker when local Deborah number  $\lambda$  is increased. Skin friction is an increasing function and reduced Nusselt number and Sherwood number are decreasing functions of local Deborah number  $\lambda$ .
- 5. For higher values of Biot number (Bi), the velocity, temperature decreases, actual concentration reduces. Increase in non-linear density  $\mathrm{ratio}(\beta)$  leads to a rise in velocity, actual concentration and a fall in temperature .Skin friction reudces, Nu and Sh enhance with larger values of Bi and  $\beta$ .
- 6. Impact of Brownian motion(Nb) and thermophoretic diffusion (Nt)on nanoparticle volume fraction is opposite in a qualitative sense. Velocity and temperature reduce with Brownian motion(Nb) and enhance with themophoresis (Nt). Skin friction enhances with Nb and Nt. Nu enhances with Nb and reduces with Nt while reversed effect is noticed in Sh with Nb and Nt.
- 7. Increase in space/temperature dependent heat source parameter(A1,B1)enhance the velocity, temperature and reduces the actual concentration. Rate of heat and mass transfer reduces with space dependent heat source while opposite effect is noticed with rising values of heat generating source. Nu and Sh enhance with A1<0,B1<0 on the wall.
- 8. Increase in chemical reaction parameter( $\gamma$ ) upsurges velocity, temperature and diminishes the actual concentration. Rate of heat and mass transfer grows on the wall in the generating chemical reaction case and reduces in degenerating case.
- 9. Lesser the molecular diffusivity(Sc)smaller the velocity, temperature and larger the actual concentration while an increase in radiation absorption (Q1) reduces the velocity, actual concentration, enhances the temperature in the flow region. Nu and Sh grow with rising values of Sc and Q1.
- 10. Velocity, temperature enhances with higher values of Prandtl number(Pr) and reduces with rising values of index number(n). The actual concentration reduces with Pr and n. Rate of heat and mass transfer decay with Pr and n.
- 11. The problem reduces to the case of Newtonian nanofluid by substituting  $\lambda = 0$ .

#### **5.REFERENCES:**

- 1 J. Harris, Rheology and Non-Newtonian Flow (Longman, London, 1977).
- 2 K. Sadeghy, A. H. Najafi, and M. Saffaripour, "Sakiadis flow of an upper-convected Maxwell fluid," Int. J. Nonlinear Mech. 40, 1220-1228 (2005).
- 3 K. Sadeghy, H. Hajibeygi, and S. M. Taghavi, "Stagnation point flow of upper-convected Maxwell fluids," Int. J. Non-Linear Mech. 41, 1242–1247 (2006).
- 4 M. Kumari and G. Nath, "Steady mixed convection stagnation-point flow of upper convected Maxwell fluids with magnetic field," Int. J. Nonlinear Mech. 44, 1048-1055 (2009).
- 5 T. Hayat, Z. Abbas, and M. Sajid, "MHD stagnation-point flow of an upper-convected Maxwell fluid over a stretching surface," Chaos Solitons and Fractals 39, 840-848 (2009).
- 6 V. Aliakbar, A. Alizadeh-Pahlavan, and K. Sadeghy, "The influence of thermal radiation on MHD flow of Maxwellian fluids above stretching sheets," Comm. Nonlinear Sci. Num. Simul. 14, 779-794 (2009).
- 7 B. Raftari and A. Yildirim, "The application of homotopy perturbation method for MHD flows of UCM fluids above porous stretching sheets," Comp. Math. Appl. 59, 3328-3337 (2010).
- 8 T. Hayat, M. Mustafa, and S. Mesloub, "Mixed convection boundary layer flowover a stretching surface filled with a Maxwell fluid in presence of Soret and Dufour effects," Z. Naturforsch. 65a, 401-410 (2010).
- 9 T. Hayat, M. Awais, and M. Sajid, "Mass transfer effects on the unsteady flow of UCM fluid over a stretching sheet," Int. J. Moder. Phys. B 25, 2853-2878 (2011).
- 10 S. Mukhopadhyay, "Heat transfer analysis of the unsteady flow of a Maxwell fluid over a stretching surface in the presence of a heat source/sink," Chin. Phys. Let. 29 (2011) DOI: 10.1088/0256-307X/29/5/054703.
- 11 M. S. Abel, J. V. Tawade, and M. M. Nandeppanavar, "MHD flow and heat transfer for the upper-convected Maxwell fluid over a stretching sheet," Meccanica 47, 385-393 (2012).
- 12 T. Hayat, M. Mustafa, S. A. Shehzad, and S. Obaidat, "Melting heat transfer in the stagnation-point flow of an upper convected Maxwell (UCM) fluid past a stretching sheet," Int. J. Numer. Meth. Fluids 68, 233-243 (2012).
- 13 S. Shateyi, "A new numerical approach to MHD flow of a Maxwell fluid past a vertical stretching sheet in the presence of thermophoresis and chemical reaction," Bound. Val. Prob. 196 (2013) DOI: 10.1186/1687-2770-2013-196.
- 14 A. Mushtaq, M. Mustafa, T. Hayat, and A. Alsaedi, "Effect of thermal radiation on the stagnation-point flow of upperconvected Maxwell fluid over a stretching sheet," J. Aerosp. Engg. 27, 04014015 (2014).
- 15 L. J. Crane, "Flow past a stretching plate," Zeitschrift Fur Angewandte Mathematik Und Physik 21, 645-657 (1970).
- 16E. Magyari and B. Keller, "Heat and mass transfer in the boundary layers on an exponentially stretching continuous surface," Journal of Physics D: Applied Physics 32 (1999) doi: 10.1088/0022-3727/32/5/012.
- 17 E. M. A. Elbashbeshy, "Heat transfer over an exponentially stretching continuous surface with suction," Arc. Mech. 53, 643-651 (2001).
- 18 S. K. Khan and E. Sanjayanand, "Viscoelastic boundary layer flow and heat transfer over an exponential stretching sheet," Int. J. Heat Mass Transf. 48, 1534-1542 (2005).
- 19 M. Sajid and T. Hayat, "Influence of thermal radiation on the boundary layer flow due to an exponentially stretching sheet," Int. Commun. Heat Mass Transf. 35, 347-356 (2008).
- 20 K. Bhattacharyya, "Boundary layer flowand heat transfer over an exponentially shrinking sheet," Chin. Phys. Lett. 28 (2011) doi: 10.1088/0256-307X/28/7/074701.

- 21 M. Mustafa, T. Hayat, and S. Obaidat, "Boundary layer flow of a nanofluid over an exponentially stretching sheet with convective boundary conditions," Int. J. Num. Meth. Heat & Fluid Flow 23, 945-959 (2013).
- 22 A. Mushtaq, M. Mustafa, T. Hayat, M. Rahi, and A. Alsaedi, "Exponentially stretching sheet in a Powell-Eyring fluid: Numerical and series solutions," Z. Naturforsch. 68a, 791-798 (2013).
- 23 I. C. Liu, H. H. Wang, and Y. F. Peng, "Flow and heat transfer for three-dimensional flowover an exponentially stretching surface," Chem. Eng. Comm. 200, 253-268 (2013).
- 24 Z. Abbas, T. Javed, N. Ali, and M. Sajid, "Flow and heat transfer of Maxwell fluid over an exponentially stretching sheet: A non-similar solution," Heat Transf. Asian Res. 43, 233-242 (2014).
- 25 T. Hussain, S. A. Shehzad, T. Hayat, A. Alsaedi, F. Al-Solami, and M. Ramzan, "Radiative hydromagnetic flow of Jeffrey nanofluid by an exponentially stretching sheet," PLoS ONE 9 (2014) doi: 10.1371/journal.pone.0103719.
- 26 K.V.Wong and O. D. Leon, "Applications of Nanofluids: Current and Future," Advan. Mech. Engg. 2010 Article ID 519659.
- 27 J. Buongiorno, "Convective transport in nanofluids," ASME J. Heat Transf. 128, 240–250 (2006).
- 28 A. V. Kuznetsov and D. A. Nield, "Natural convective boundary-layer flow of a nanofluid past a vertical plate," Int. J. Therm. Sci. 49, 243-247 (2010).
- 29 D. A. Nield and A. V. Kuznetsov, "The Cheng–Minkowycz problem for natural convective boundary-layer flow in a porous medium saturated by a nanofluid," Int. J. Heat Mass Transf. 52, 5792-5795 (2009).
- 30 W. A. Khan and I. Pop, "Boundary-layer flow of a nanofluid past a stretching sheet," Int. J. Heat Mass Transf. 53, 2477-2483 (2010).
- 31 M. Mustafa, T. Hayat, I. Pop, S. Asghar, and S. Obaidat, "Stagnation-point flow of a nanofluid towards a stretching sheet," Int. J. Heat Mass Transf. 54, 5588-5594 (2011).
- 32 M. Mustafa, M. A. Farooq, T. Hayat, and A. Alsaedi, "Numerical and series solutions for stagnation-point flow of nanofluid over an exponentially stretching sheet," PLoS ONE 8 (2013) doi: 10.1371/journal.pone.0061859.
- 33 M. Mustafa, T. Hayat, and A. Alsaedi, "Unsteady boundary layer flow of nanofluid past an impulsively stretching sheet," J. Mech. 29, 423-432 (2013).
- 33a.M.Mustafa,Junaid Ahmad Khan,T.Hayat and A,Alsaed:Simulations for Maxwell fluid flow past a convectively heated exponentially stretching sheet with nanoparticles.,AIP ADVANCEs,V.5,037133(2015)
- 34O. D. Makinde, W. A. Khan, and Z. H. Khan, "Buoyancy effects on MHD stagnation point flow and heat transfer of a nanofluid past a convectively heated stretching/shrinking sheet," Int. J. Heat Mass Transf. 62, 526-533 (2013).
- 35 A. V. Kuznetsov and D. A. Nield, "Natural convective boundary-layer flow of a nanofluid past a vertical plate: A revised model," Int. J. Therm. Sci. 77, 126-129 (2014).
- 36M. Mustafa, M. Nawaz, T. Hayat, and A. Alsaedi, "MHD boundary layer flow of second grade nanofluid over a stretching sheet with convective boundary condition," J. Aerosp. Engg. 27, 04014006 (2014).
- 37 A. Mushtaq, M. Mustafa, T. Hayat, and A. Alsaedi, "Nonlinear radiative heat transfer in the flow of nanofluid due to solar energy: A numerical study," J. Taiwan Inst. Chem. Eng. 45, 1176-1183 (2014).
- 38 M. M. Rashidi, N. Freidoonimehr, A. Hosseini, O. A. Beg, and T. K. Hung, "Homotopy simulation of nanofluid dynamics from a non-linearly stretching isothermal permeable sheet with transpiration," Meccan. 49, 469-482 (2014).

- 39 M. M. Rashidi, S. Abelman, and N. Freidoonimehr, "Entropy generation in steady MHD flow due to a rotating porous diskin a nanofluid," Int. J. Heat Mass Transf. 62, 515-525 (2013).
- 40 M. Turkyilmazoglu, "Unsteady convection flow of some nanofluids past a moving vertical plate with heat transfer," ASME J. Heat Transf. 136, 031704 (2013) doi: 10.1115/1.4025730.
- 41 M. Turkyilmazoglu and I. Pop, "Heat and mass transfer of unsteady natural convection flowof some nanofluids past a vertical infinite flat plate with radiation effect," Int. J. Heat Mass Transf. 59, 167-171 (2013).
- 42 M. Sheikholeslami and M. Gorji-Bandpy, "Free convection of ferrofluid in a cavity heated from below in the presence of an external magnetic field," Powder Technol. 256, 490-498 (2014).
- 43 M. Sheikholeslami, M. Gorji-Bandpy, D. D. Ganji, and S. Soleimani, "Thermal management for free convection of nanofluid using two phase model," J. Mol. Liq. 194, 179-187 (2014).
- 44 M. Sheikholeslami, D. D. Ganji, M. Gorji-Bandpy, and S. Soleimani, "Magnetic field effect on nanofluid flow and heat transfer using KKL model," J. Taiwan Inst. Chem. Eng. 45, 795–807 (2014).
- 45 J. A. Khan, M. Mustafa, T. Hayat, M. Asif Farooq, A. Alsaedi, and S. J. Liao, "On model for three-dimensional flow of nanofluid: An application to solar energy," J. Molec. Liqui. 194, 41-47 (2014).
- 46 M. Mustafa, A. Mushtaq, T. Hayat, and B. Ahmad, "Nonlinear radiation heat transfer effects in the natural convective boundary layer flow of nanofluid past a vertical plate: A numerical study," PLoS ONE 9 (2014) doi: 10.1371/journal.pone.0103946.